Chapter 1
Signature of Active Tectonics and Its Implications Towards Seismic Hazard in Western Part of Stable Peninsular India

Kapil Mohan, Naveen Kumar, Rakesh Dumka, and Sumer Chopra

Abstract The Dadra-Nagar Haveli and the surrounding region, in western India, have been facing moderate seismicity since 1856. Two historic events (Magnitude Ms 5 in 1935 and Magnitude Ms 5.7 in 1856) were reported in the past in this region. Additionally, more than 200 earthquakes ($1.0 \leq M \leq 5.7$) were also reported between M 1 and 5.7 in this area. The epicentre of these earthquakes follows the trend of the faults mapped in the study area. Current study is aimed to map the tectonic features in the region and their associated tectonic-geomorphic features to infer the tectonic behaviour and their impact on seismic hazard in the western part of India. The RIAT of the watersheds of main rivers has been estimated through the analysis of geomorphic indices like stream length (SL) gradient, hypsometric integral (HI), basin shape (BS) and valley floor (VF) and three classes (class II high ($1.3 \leq RIAT < 1.5$), class III—moderate ($1.5 \leq RIAT < 1.8$), and class IV—low ($1.8 \leq RIAT$)) have been found in the study area indicating it a seismically active region. The study area falls within the Panvel seismic zone and the recent seismicity has also been witnessed in the vicinity of N-S trending linear geological features. The presence of seismicity, faults with slickenside planes, shear zones with brittle nature, deformed dykes and extensional features suggests that the region has faced neotectonic activities and is even now active seismically. Through geological fieldwork, the evidence of past major seismic events (>5.5) is also found well preserved in the form of SSDS/seismites in quaternary sediments. The identified SSDS/seismites are mostly formed within the sandy silt, sandy gravel and clay beds; and include sills, dykes, suspended clast blocks, slump structures, and convolute bedding. The extent and dimension of these seismites indicate that the mechanism to trigger these and forces driven for

K. Mohan
National Center for Seismology, Ministry of Earth Sciences, New Delhi, India

N. Kumar (✉) · R. Dumka · S. Chopra
Institute of Seismological Research, Knowledge Corridor, Gandhinagar, Gujarat, India
e-mail: naveen5attri@gmail.com

N. Kumar
EDRC Hydel & Tunnels Larsen and Toubro Limited, Faridabad, India

Sandeep et al. (eds.), *Geohazards*, Advances in Natural and Technological Hazards Research 53, https://doi.org/10.1007/978-981-99-3955-8_1

the source of these features are shock waves of earthquake. The maximum moment magnitude of Mw 6.2 has been estimated based on the maximum displacement recorded along the normal active fault mapped in the study area, which trends N170°–N350°, with a sharp dip of 72° in the SW direction. The seismic hazard assessment of the area considering scenario earthquake of Mw 6.2 along this fault located east of Silvasa city has been estimated using the Stochastic Finite Fault Modelling simulation technique. A maximum peak ground acceleration (PGA) of the order of ~0.44 g has been assessed in the area with a maximum site amplification of 2.15.

Keywords Panvel seismic zone · Relative index of active tectonics · Soft sediment deformation · Seismic hazard assessment

1.1 Introduction

Neotectonics and active tectonics are the key geological agents, which are responsible for the modelling of present-day geomorphology on the earth. The tectonic processes are responsible for the many geological hazards to society. Among all the geological hazards, earthquakes have the most disturbing effect on society. In the field of earth science, the tectonic geomorphology is a rising domain due to its addition of distinctive tools like geodetics, geomorphology, geochronology. Additionally, these tools help in assessment of the deformation rate, incision upliftment, erosion and fault slip rates (Kumar et al. 2020b).

For a long time, the peninsular shield of India has been considered stable seismically and the region has the potential of generating only low-level seismicity at few places (De Montessus de Ballore 1911; Tandon and Chatterjee 1968; Krishnan 1968). However, this belief has been shattered after the occurrence of the 1967, Koyna Earthquake of M 6.2. The M 6.2 magnitude Koyna earthquake forced researchers to reconsider and reassess the seismic status of Peninsular India. The detailed studies conducted by (Chandra 1977; Auden 1949; Watts and Cox 1989; Bansal and Gupta 1998; Dole et al. 2000; Rajendran 1997; Sheth, 1998; Raj et al. 2003; Mohan et al. 2007; Kaplay et al. 2013, 2016; Naik and Awasthi 2003; Kale et al. 2016; Jade et al. 2017, Kumar et al. 2022, 2020a, b) show that, PFS zone, the Konkan coastal belt, Koyna are affected by tectonically generated deformation activities in the Deccan Volcanic region.

The profound accessibility of Geographic Information System and their role in the uninterpretation of digital elevation models has helped to the purposes of RIAT evaluation by means of geomorphic indices. The research on this subject are growing and have seen significant growth in last decades (Kumar et al. 2022). The GIS-based software enables to extract and analyse of landscapes with detailed information. The Assessment of RIAT from indices of geomorphic shows the rates of upliftment and deformation in the landscapes for the long time (Bull 1977; Kumar et al. 2022).

The current area under study is situated in western portion of DVP in the Western India (Fig. 1.1). Since late Triassic/early Jurassic to late Cretaceous periods, West

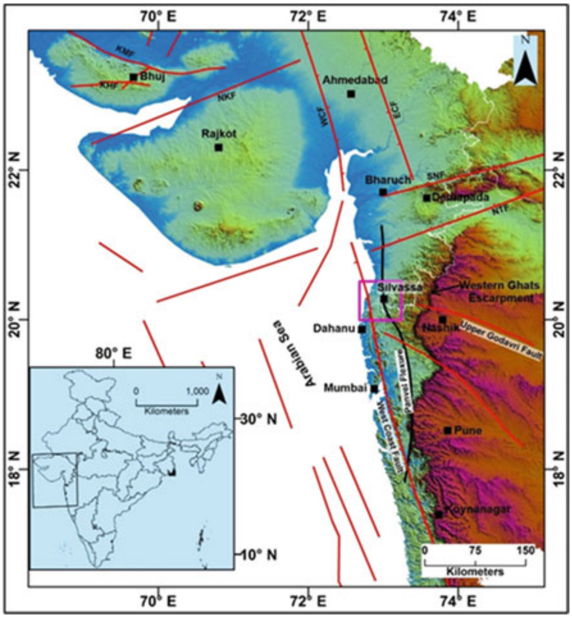

Fig. 1.1 The Tectonic map of Western India (after Biswas 1982; Sheth 1998), KMF-Kachchh Mainland Fault, KHF-Katrol Hill Fault, ECF-East Cambay Fault, WCF-West Cambay Fault, NKF-North Kathiawar Fault, SNF-Son-Narmada Fault, NTF-North Tapti Fault

Coast of India has evident persistent rifting events. The current study area is situated in the Panvel flexure seismic zone (Fig. 1.1), which is undergoing through earthquake events later 1618 (Rao 2005; Rao and Rao 1984; Kumar et al. 2020a) (https://isr.gujarat.gov.in/). Key purpose of this research is to evaluate the seismic hazard in area as there are no considerable studies associated to active tectonic and seismic hazard due active fault (s) in the area under study.

1.2 Geological Setting and Study Area

The area under study is situated in western parts of India (Fig. 1.1). In the west, it's confined by WCF (west coast fault), whereas in east is bounded by Western Ghats escarpment and the central portion is occupied by the Panvel flexure (Fig. 1.1). The Deccan basalt, trachyte and rhyolite complex dominates the study area with basic rock dykes. The central parts of the study area are occupied by alluvium these sediments are distributed in intermittent spots of major rivers (Kumar et al. 2022 and 2020a, b). During Pliocene, the Western Coast of is formed due to the faulting (Krishnan 1953). The WCF is the main tectonic structure in this part of India. Due to its NNW-SSE trend, the straight orientation in the west coast and up to the Gulf of Cambay in the north and continue to the south of Mumbai is considered to be due to this fault (Bombay) (Krishnan 1982).

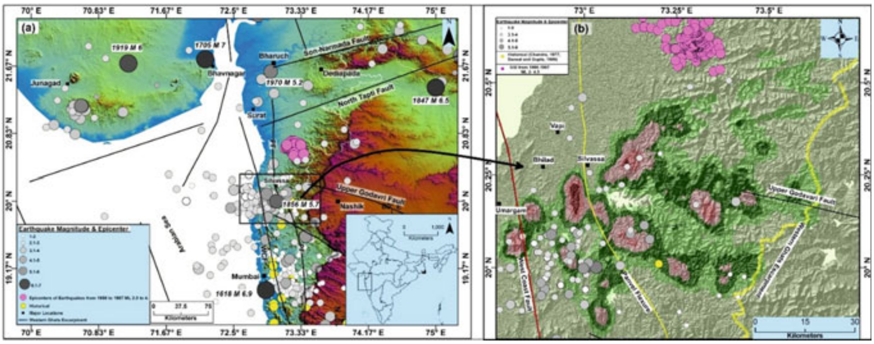

Fig. 1.2 **a** The Seismotectonic map of western India **b** The Seismotectonic map of the study area (After Kumar et al. 2020b)

1.3 Seismotectonics of the Study Area

The area is experiencing earthquakes since 1856. Two historical events (M_S5 in 1935 and M_S5.7 in 1856) were recorded in the study area especially concentrated in the southern part (Kumar et al. 2020b; Bansal and Gupta 1998; Chandra 1977). At present, the seismicity in the region endorses the active nature of the present tectonic features; epicentres of the earthquakes are focussed beside these tectonic units (Kumar et al. 2020a). A substantial number of earthquakes between M1 to 5.7 (Chandra 1977; Bansal and Gupta 1998 and Kumar et al. 2020b) are documented in the area under study. The disruption due to the tectonism is even now marked by several earthquakes in western India (Fig. 1.2).

1.4 Methodology

The targeted research work is distributed into three parts (i) evaluation of RIAT, (ii) soft-sediment deformation study and (iii) estimation of seismic hazard due to an active segment of the fault.

1.4.1 Evaluation of RIAT

For evaluation of the RIAT, the remote sensing (RS) and geographic information system (GIS) techniques are used. The network of streams and the demarcation of watershed boundaries are done utilizing Survey of India toposheet at 1:50,000 and SRT Digital Elevation Models (30 m) in the GIS system. The recognition of linear feature like faults, lineaments and dykes, processing of image, production of the FCC, and preparation of shaded relief maps are prepared. The indices, i.e., Bs, HI, SL, Vf, are assessed and after calculation of all, sub-watersheds are classified in three category on the basis of the value of index. Finally, these values are added and each every sub-watershed has been grouped according to the value of the RIAT (Relative Index of Active Tectonics).

1.4.2 Soft Sediments Deformation (SSD) Structures

The study related to seismite (SSDS) is completed in the steps as follows:—seismites are identified, mapped in alluvial sediments pile up along Damanganga river banks in the study area. These seismites were measured and their association with the surrounding layers of sediments was done. Then the literature related to the seismites has been reviewed and the reasons (whether primary or secondary) behind the formation of these seismites are studied. In addition, the mechanism of trigger, the earthquake distribution and the manifestation of active faults in the region have been investigated.

1.4.3 Seismic Hazard Assessment Due to Active Fault Segment

To determine the seismic hazard of any area, the future earthquake potential valuation is mandatory. Precisely, it is essential to estimate the size of the earthquakes that might be produced by any specific fault. The magnitude of earthquake may be related to rupture parameters like length and displacement (Iida 1959; Tocher 1958; Chinnery 1969). To estimate these parameters, prior paleo-seismic and geologic studies of active faults are required. The parameters/data from the geological and geomorphic studies can be used to evaluate the time of historical earthquakes, the extent of displacement of each event, and the segmentation of the fault zone (Schwartz and Coppersmith 1986; Schwartz 1988; Coppersmith 1991) in the study area. To interpret these source features into estimates of earthquake size, the empirical relationship between rupture parameters and the measure of earthquake size, typically magnitude, is required (Wells and Coppersmith 1994).

Numerous published realistic relationships are available to relate magnitude to various fault rupture parameters, like fault rupture displacement versus rupture length and magnitude versus rupture area (subsurface and surface both), magnitude contrasted with total fault length (Tocher 1958; Iida 1959; Albee and Smith 1966; Chinnery 1969; Ohnaka 1978; Slemmons 1977, 1982; Acharya 1979; Bonilla and Buchanon 1970). There are research works also available that relate the seismic moment and magnitude to the rupture length, width, and an area of the rupture (as assessed from the amount of deformations at surface, the aftershock zone extent, or functions of earthquake source time) (Utsu 1970; Kanamori and Anderson 1975;

Wyss 1979; Singh et al. 1980; Purcaru and Berckhemer 1982; Darragh and Bolt 1987). The empirical relationships proposed by Wells and Coppersmith (1994) were well-tested and used in a number of significant studies in the seismic Hazard Assessment (Mohan et al. 2017, 2018, 2021). Therefore, the same relationship has been used in the present study to estimate the earthquake magnitude from the observed displacement, estimation of rupture area, rupture length and rupture width. The details are as follows.

1.4.3.1 Maximum Earthquake Magnitude

The length of surface rupture and the maximum displacement on continental fault traces are the most commonly used parameters to conclude magnitudes for paleo-earthquakes (Wells and Coppersmith 1994). Here, we have used the maximum displacement method (Wells and Coppersmith 1994) to calculate the maximum magnitude of an earthquake along the identified faults present in the study area.

Maximum Displacement Method

The maximum displacement method involves determining the maximum displacement (MD) estimated from the paleoseismological investigations associated with a paleoearthquake, and comparing that value to the maximum displacement measured or computed for an instrumentally recorded earthquake (Wells and Coppersmith 1994).

The empirical relationship between Moment magnitude (M) and MD will have the form of:

$$M = a + b * \log(MD)$$

Regressions coefficient derived by Wells and Coppersmith (1994) for Moment magnitudes (M) and maximum displacement (MD) are:

$$a = 6.69 \text{ and } b = 0.74$$

Along the normal active faults mapped in the study area, the maximum surface displacement of ~0.25 m is measured. Thus in the above equation with MD = 0.25, the possible Moment magnitude of Mw 6.2 is estimated.

1.4.3.2 Estimation of Seismic Hazard

The seismic hazard can be estimated using two different methodologies (i) Deterministic Seismic Hazard Assessment and (ii) Probabilistic Seismic Hazard Assessment.

In the case of seismic designing and retrofitting of structures, the DSHA has an advantage (McGuire 2001). The DSHA is also useful to check the worst-case scenarios (the largest magnitude at the closest distance) and in the training and plans for emergency response and post-earthquake recovery (McGuire 2001).

In the present study, the deterministic seismic hazard assessment has been conducted to estimate the seismic hazard due to the active segment of the Kilvani Fault (Fig. 1.3), where a displacement of 0.25 m was observed. The Strong motion simulation involves the rigorous mathematical exercise covering the earthquake source/rupture (geometry, nucleation, and propagation) and seismic wave propagation (between the source to the site) through different rock boundaries in the earth's crust. While passing through different subsurface layers, the seismic waves change (amplifies/deamplifies) and reach the site. Cancani (1904) initiated the simulation of strong motion (SM) by generating the SM parameters from the seismic intensity. Later on, Housner (1947) proposed the concept of black-box simulation for simulating SM by using white Gaussian noise. Presently, mainly five types of SM simulation techniques are available. These are (1) composite source modelling (Saikia and Herrmann 1985; Saikia 1993; Zeng et al. 1994; Yu 1994; Yu et al. 1995), (2) stochastic simulation (Boore 1983; Lai 1982; Boore and Atkinson 1987), (3) empirical Green function technique (EGF) (Hartzell 1978, 1982; Hadley and Helmberger 1980; Kanamori 1979; Mikumo et al. 1981; Irikura and Muramatu 1982; Irikura 1983, 1986; Muguia and Brune 1984; Hutchings 1985; Kamae and Irikura 1998; Irikura and Miyake 2011), (4) semi-empirical approach (Midorikawa 1993; Joshi and Midorikawa 2004; Joshi et al. 2001; Mohan 2014), and (5) Stochastic Finite Fault Source Modeling Technique (SFFMT) (Motazedian and Atkinson 2005). Every simulation technique follows certain conditions for the assumptions of source, path, and site effects and rarely estimates all three in one step. Due to advancements in the research methodologies, the SM simulation can be effectively done by dividing it into three major parts (i) source characterization and rupture propagation, (ii) wave propagation from source to base rock/Engineering bedrock (EBR), and (iii) wave propagation from EBR to surface considering near-surface effects gathered in the form of site amplification from geotechnical or/and geophysical parameters like Vs. Generally, one can choose any technique based on available input parameters (source, path and site conditions). The SFFMT is a well-tested SM technique of simulation and well tested in Gujarat by Chopra et al. (2010, 2013), Mohan et al. (2017, 2018, 2021) for seismic hazard assessment. In view of this, the technique has been selected to estimate the strong motion at a grid interval of 10 km × 10 km. A significant portion of the study area is covered with sediments. The United State Geological Survey (USGS) provided the worldwide Vs30 values based on the topographic slope (Allen and Wald 2009). The Vs30 values in the study region vary from 250 m/sec to 900 m/sec. Therefore, the strong motion has been simulated at B/C Boundary at Vs30 of 760 m/sec and crustal amplifications suggested by Boore and Joyner (1997) for the Vs30 of 760 m/sec. The near-surface wave attenuation/Fall-off of the high frequency (>1 Hz) Fourier amplitude spectrum (Anderson and Hough 1984)/Kappa values (κ) is taken as 0.03 as used by Chopra et al. (2010) for the estimation of seismic hazard in the adjacent Mainland Gujarat. The Quality factor and stress drop

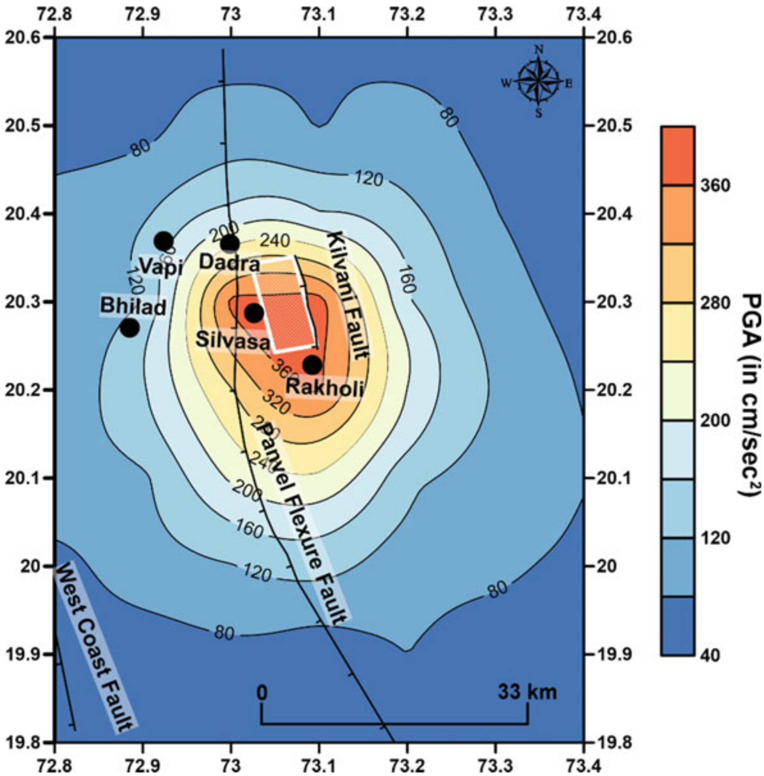

Fig. 1.3 The PGA (in cm/sec^2) distribution map at a Vs of 760 m/sec due to an earthquake of M_w6.2 along the Kilvani Fault

were also considered as suggested by Chopra et al. (2010) for the adjacent Mainland Gujarat area. The input parameters considered for the simulation of ground motion are given in Table 1.1.

Site amplification plays a significant role in the estimation of seismic hazards in any area. In the study area, the Vs30 values proposed by USGS have been used to estimate the site amplification factors at a grid interval of 10 km × 10 km by using the velocity–amplification relationship proposed by Matsuoka and Midorikawa (1994). The PGA distribution map thus prepared at Vs30 of 760 m/sec, the site amplification map (between the Vs of 760 m/sec and the surface Vs) and the PGA distribution map at the surface level have been shown in Figs. 1.3, 1.4, and 1.5, respectively.

Table 1.1 The selected model parameters for the simulation of ground motion

Magnitude (Mw)	6.2	
Fault length and width (km)	(17 km and 11 km)	Wells and Coppersmith (1994)
Strike and dip	170° and 72°	
Slip distribution	Random	
Shear wave velocity	3.6 km/sec	Chopra et al. (2010)
Stress drop	100 bars	Chopra et al. (2010)
Kappa	0.03	Chopra et al. (2010)
Anelastic attenuation Q(f)	$118f^{0.65}$	Chopra et al. (2010)
Geometric spreading	1/R (R≤40 km)	Bodin et al. (2004)
	$1/R^{0.5}$ (40≤R≤80 km)	
	$1/R^{0.55}$ (R≥80 km)	
Duration properties	fc^{-1} (R < 10 km)	Atkinson and Boore (1995)
	fc^{-1} + 0.16R (10≤R≤70km)	
	fc^{-1} - 0.03 (70<R≤130 km)	
	fc^{-1} + 0.04R (130<R<1000 km)	

1.5 Result and Discussions

1.5.1 Faults and Lineament Mapping

During the field geological mapping, a normal fault has been mapped near Kilvani village trending N170°–N350°, with a sharp dip of 72° in the SW direction (Fig. 1.6a). It is evident by the impressive growth of slickensides, the slickensides were occupied by fine-grained white zeolites and calcite. The slickensides zone is very well visible in a depth of 2–4 m in road cuttings (Fig. 1.6a). The slickenlines are suddenly tending towards the south-SW on the surface of fault. The smoothness in touch in the downward direction on slickeside surface and upward direction roughness is observed (Fig. 1.6b), which suggests that the missing western block moved down relative to the block east of the fault (Doblas 1998; Argles 2010). The exposed bedrock along the rock cutting is mainly Basalt, which is found sheared and very closely spaced fractures are formed due to the faulting. The presence of normal fault with a trend N170°–N350° dipping 72° SW suggests the NE-SW extension in the

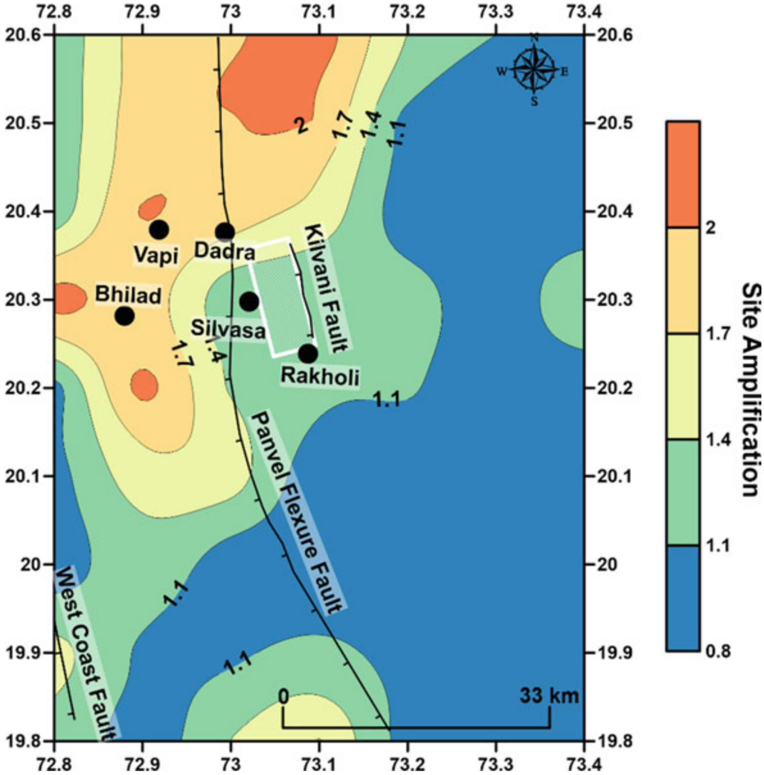

Fig. 1.4 The site amplification map of the study area

study area. The slickensides on striated fault planes were recorded in the expose rock section at Kilvani and Meghwal, (Fig. 1.6). Generally, they present on fresh outcrops showing, thin (~1–5 mm), mineralized (secondary zeolite and quartz, and calcite.) the planes of fault that display primarily a normal slip. Mineralized layers are likely to erode (Doblas 1998; Whiteside 1986; Kranis 2007). The Kilvani fault is the younger fault in the study area as along this fault the displacement in the sediments has been mapped. Though other faults (like the WCF and PF) are also present in the region but along these faults, the signature of displacement or movement has not been found in the study area. The Kilvani Fault also follows the trend of the major faults and the epicentres are occurring along the trend of these faults. Therefore, to estimate the hazard related to seismic event in the area and to estimate the maximum seismic potential, the Kilvani Fault has been considered.

The lineament map has also been generated in the study area, and the results of the analysis depict that these lineaments display maximum resemblance with the trend of the tectonic features present in the area. The lineament density analysis was performed in GIS platform by dividing the study area into four sectors, the results of the lineament density analysis show that the highest density of the lineaments is

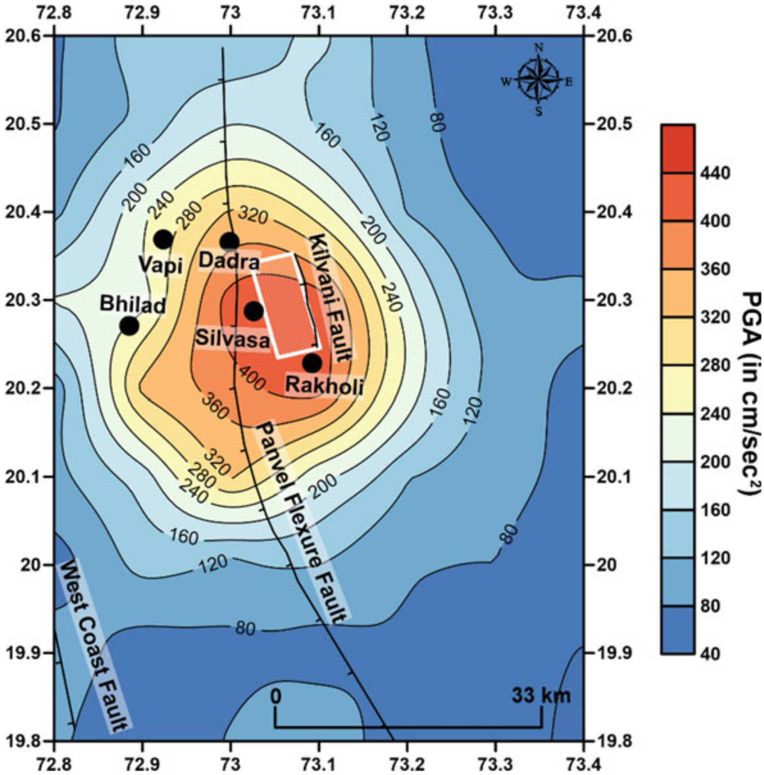

Fig. 1.5 The PGA (in cm/sec^2) distribution map of the surface level due to earthquake of M_W6.2 along the Kilvani Fault

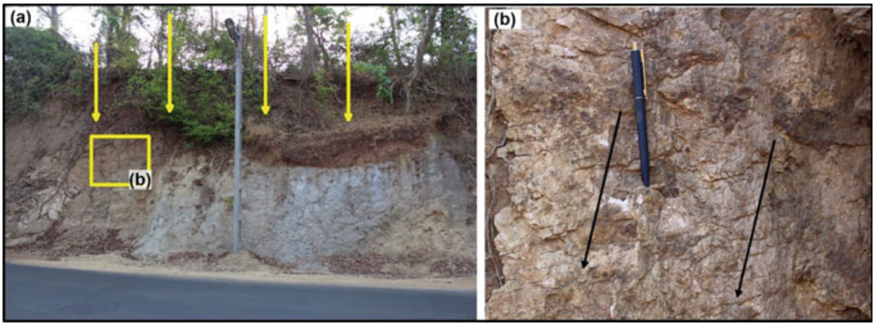

Fig. 1.6 **a** Normal fault near Kilvani village (20°18′1.70"N, 73° 5′53.55"E) road exposures with strike N170°–N350° and dip amount 70° in SW direction, **b** Slickensided fault plane showing the direction of movement by black arrows (After Kumar et al. 2020b)

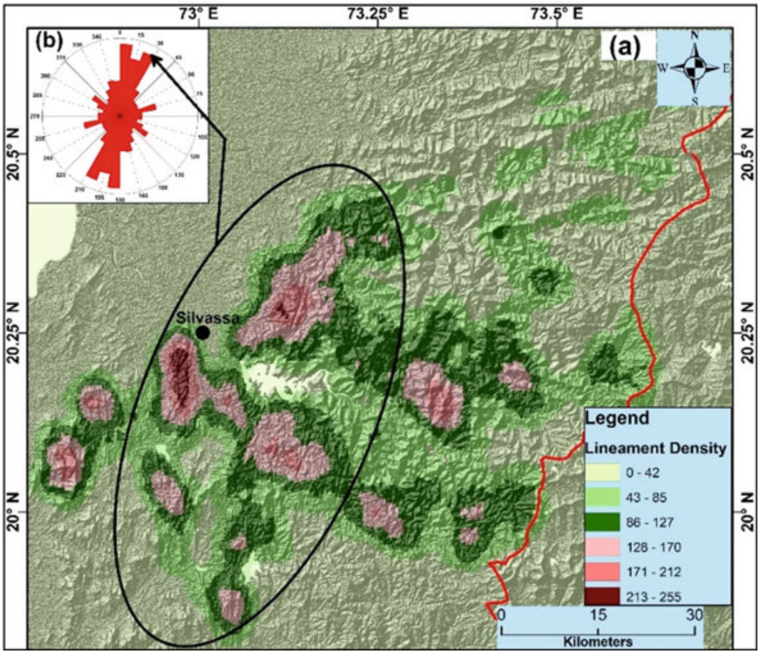

Fig. 1.7 Structural lineament map of the area: **a** lineament density map in which the flat area shows low concentration as compared to flanks, **b** rose diagram of lineaments with a major trend in N-S direction (inset) (After Kumar et al. 2020b)

in the central portion of the study area along the axis of the Kilvani Fault and other tectonic features (Fig. 7b), while the lowest lineament density in alluvial portion. The high lineament density (Fig. 7b) observed in the central portion (in a black circle) was linked with the regional tectonic features present in the study area. Furthermore, the interpretation of the rose diagram and overlay investigation shows that maximum lineaments/linear geological structures are aligned to sub-parallel (N–S direction) to the Kilvani Fault and other tectonic structures (Fig. 7b inset).

1.5.2 Relative Index of Tectonic Activities

The indices like stream length index, valley to floor ratio, hypsometric integral, and basin shape index are calculated, and their collective results were combined to assess the relative index of tectonic activity (RIAT) in the study area. The stream length is an important tool to estimate the relative tectonic activities of any area. The aberration in the profile of river from the steady state may be due to the effect of the lithological, or climatic and tectonic reasons (Hack 1973). The SL index value has been estimated and the area is distributed into 54 sub-basins. Based on the results and the values classified into three classes; Class I (SL, ≥ 600), Class II (300, < SL < 600), and Class III (SL, ≤ 300). The 07 numbers of sub-basins come in class-I, a sum of 10 sub-basins comes in class-II and 10 sub-basins comes in Class-III. The results of the study disclose the presence of moderate and high activities in the eastern and northern portions, individually. The central and western portion is moderately least tectonically active along with fairly high stream length index value. The valley to floor ratio index is measured to differentiate among V and U shaped valleys. These are (V-shaped) developed in response to upliftment and flat-floored (U-shaped) wide valleys formed as a reaction to the stability of base level (Bull 1977). The incision by river results into uplift,emt, while low Vf is associated to progressive incision rate and uplift. The < 1 Vf value is related to the V-shaped valleys, linear streams shape with and revealed active upliftment and non-stop downgrade cutting. The > 1 Vf value is associated to flattened or valleys with U shaped, which displays attainment of erosion of base level mainly in response to relative tectonic inactivity (Keller 1986; Keller and Pinter 2022). In the region, the valley to floor width index is calculated in the main streams of sub-basins. Three numbers of classes were classified in this case also; Class I, (Vf ≤ 0.5), Class II, (0.5 < Vf < 1.0), and Class III, (Vf ≥ 1.0). The findings of the study reveal that the majority of the area comes in Class 1, which shows the V-shape and therefore discloses a remarkably higher degree of tectonic activity. The hypsometric integral index is unbiased of area of the basin and is usually consequent for a precise drainage basin. Usually, the HI outlines the elevational dispersal of an exact area of land, mainly a drainage basin (Strahler 1952). The high value of hypsometric index is possibly related to the current tectonic activity, whereas, the low values signify the mature landscapes, which have been further eroded and less affected by the recent tectonic activities (Strahler 1952). After the results of the analysis, in relations of concavity and convexity of hypsometric curve, the HI may be categorized into three classes, Class 1, (HI ≥ 0.5) shape of concave curve; Class 2, (0.4 < HI < 0.5) a shape of concave-convex curve, Class 3, (HI ≤ 0.4) the convex shape of curve. The quantity of the breadth of sub-basins varies as of one place to another hence the average value is taken to assess the shape of studied river basin. As per Elias et al., 2019, the index of basin shape (Bs) comprises three classes: (Class I) basin with Elongated shape (Bs ≥ 4); (Class II) basin with semi-elongated shape (3 ≤ Bs < 4), and (Class III) basin with Circular shape (Bs < 3) (Fig. 1.8). The results of the study reflect that high values of Bs are associated with the basins with elongated shapes, generally connected to relatively enhanced tectonic activities, and low values of Bs entitled to basins with a circular shape generally associated with low tectonic activities.

The eruption of Deccan flood basalt took place at ~65 Ma and covered > 500, 000 km^2 (Chandra 1977; Cox 1988; Acharya et al. 1998; Ramesh and Estabrook 1998). The earlier research in the Deccan province ascribed the viewed variations basically to change in climate, geomorphology, riverine systems, fluctuations in sea levels, and only devoted to the Deccan upland region connection with movements related to neotectonism (Dikshit 1970; Kale and Rajaguru 1987; Watts and Cox 1989; Widdowson and Cox 1996; Renne et al. 2015; Kale et al. 2016). In the present research, an effort is made to evaluate RIAT. The values of the

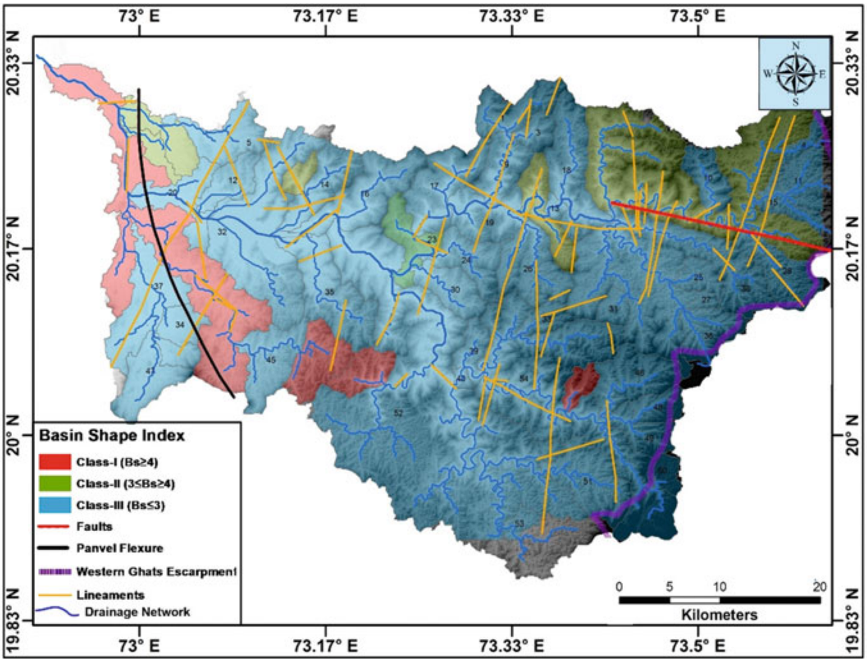

Fig. 1.8 Basin shape index distribution in the sub-watersheds in the study are (after Kumar et al. 2022)

indices computed are added to compute Relative index of Tectonic Activities and then appraised the spatial extent and dispersal of tectonic activities in the study area. The value of RIAT attained by addition of all the indices is grouped in three categories to describe the grade of RIAT in the region, which are given as: 1.3 ≤ RIAT, < 1.5 in Class II with high activities; 1.57–1.86, class III with moderate activities; and 2.0–2.33 Class IV, with low comparative tectonic activities separately. The distribution of these categories is shown in (Fig. 1.9). The river basins 44,42, 21, 2 fit in to class II (with high activities); the basins 52,43,8,4,3,1 fit into class III (with moderate activities); left all sub-basins fit into class IV (with low activities). The relative index of tectonic activities is high alongside the UGF (Upper Godavari fault), the WGE (Western Ghats escarpment), new lineaments and faults, present in the study area.

In the study area, various types of seismites also mapped from various location in the river sediments during the field investigation. The seismites are primarily found in sandy silt, silty clay and sandy gravels. Major seismites in the area include dykes of intrusive nature and sills of sediments, sediments with slumping structures, clast chunks with suspended nature and bedding with convolute shape.

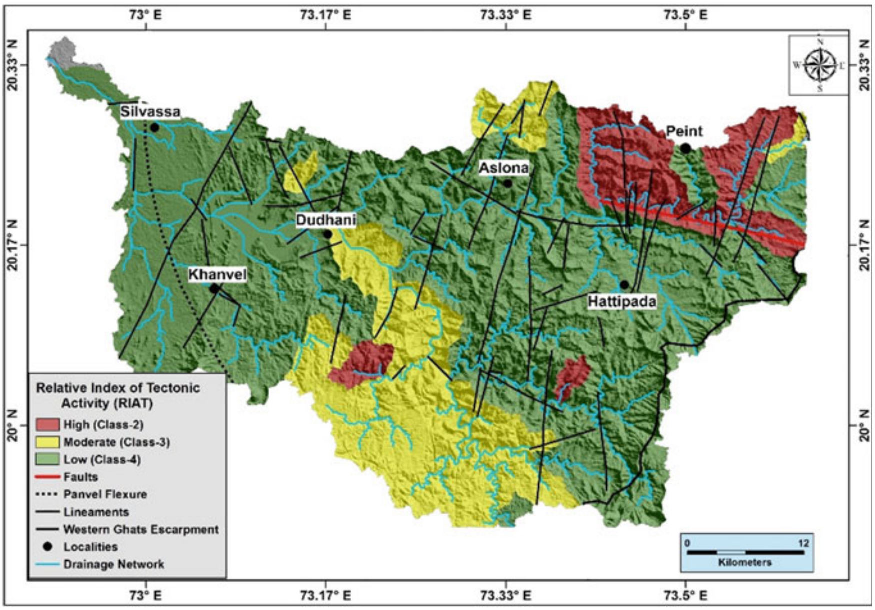

Fig. 1.9 Distribution of relative index of active tectonics (RIAT) in the Darda and Nagar Haveli and surroundings (after Kumar et al. 2022)

1.5.3 Deformation Mechanism

In previous studies in the central regions of Maharashtra the occurrence of SSDS, warping/flexures of sediments, remarkable displacement and deformation in alluvial deposits were documented (Dole et al. 2000, 2002; Rajendran 1997; Kaplay et al. 2013, 2016; Kale et al. 2016). There are various deformation mechanisms, which describe the formation of the seismites. Mills (1983), suggested that the seismites are produced by the disruption of non-lithified and sedimentary layers with water saturation. Researchers like Mills (1983), Lowe (1975), Owen (1987, 2003), Moretti and Sabato (2007) have recommended various deformation mechanisms behind the formation of seismites. The seismites may be formed by the failure in slope due to slumping, liquidization and shear stresses. It might happen if driving force results in reverse density (Allen 1982). The liquefaction or fluidization of the sediments is the most important reason in development of seismites in cohesion-less and water-rich sediment layers (Allen 1982). Normally, the process of the cause and the distortion can be instigated because of the results of exterior instruments like groundwater fluctuations, gravitational and storm currents, and an event of earthquake (Sims 1975; Lowe 1975; Owen 1987, 1996).

1.5.3.1 Trigger Mechanism

There are several probable trigger mechanisms described by various researchers most of them are summarized in this section. The commonly accepted trigger mechanisms are (a) loading of sediment (Moretti and Sabato 2007; Anketell et al. 1970), (b) storm and turbiditic currents (Molina et al. 1998; Dalrymple 1979; Alfaro et al. 2002), (c) sudden collapse in sediments (Waltham and Fookes 2003; Moretti et al. 2001; Moretti and Ronchi 2011), (d) liquefaction of soil through previous fissures (Holzer and Clark 1993; Guhman and Pederson 1992), (v) an earthquake event (Lowe 1975; Seilacher 1969; Sims 1975; Rossetti 1999; Calvo et al. 1998; Alfaro et al. 1999). In the study area, the sediment loading appears to be of least significance for features observed in the alluvial deposits within the study area. Seismites mapped in the study area are present in a large area, which recommends a further regional trigger mechanism in comparison to the limited acts of loading of sediment and storms current, collapse structures, turbiditic currents, and liquefaction via previously existing fissures. Seismic shaking due to the earthquake event could be the most plausible trigger mechanism and it might be the major reason for the development of the seismites within the study area, while present study area is bordered by faults which are active in nature (neotectonically), the Panvel Flexure Fault and its sympathetic faults. The deformed sediments found in the study area may probably be categorized as seismites, based on their extent, nature (river deposits), shapes and dimensions (Owen 1996; Sims 1975; Rossetti 1999; Calvo et al. 1998). The seismites are formed due to earthquake shock after its occurrence and for the development of these features; an area must have undergone to tectonic event and earthquake activities (Moretti and Sabato 2007; Jones and Preston 1987). The ground Shaking done by an earthquake is the widely accepted and famous phenomena behind sediment fluidization. All through the incidence of an earthquake, the pressures in pores are increased for the short time, which results into the loss of contact with grain–grain and short-term loss of strength as of limited pore water expulsion (Allen 1977). In study area, these seismites are qualified for earthquake origin on the basis of the explanations as follows: (a) undeformed beds of soil are present below and above the deformed beds; (b) the size of soil grains of deformed sediments falls in the range of soil liquefaction because of shaking due a seismic ecevnt (Balkema 1997); (c) seismites and their extent, shape, magnitudes, sedimentological properties and facies, are common to the studies on seismites by Rossetti (1999), Sims (1975), Vanneste et al. (1999) and Jones et al. (2000); (d) the presence of active faults in the present study area (Kumar et al. 2020a,b, 2022) and has been experiencing earthquakes with magnitude $M \geq 5$, thus the seismites in the alluvial soil from the area meet with key conditions to be characterized as seismites. To trigger liquefaction in the soil, an earthquake of magnitude 2–3 is enough (Seed and Idriss 1971). For causing liquefaction in the soil, an earthquake magnitude must be >4.5 (Marco and Agnon 1995). The presence of active faults within 15 km to 50 km distance of the study area also affirms the seismites of seismic origin (Fig. 1.10). In view of all the above evidence, it has been postulated that the seismites present in the study area are developed due to the earthquake event of magnitude $M \geq 5$. It has also been proposed that the earthquake, which might have generated the seismites, possibly will be between magnitude 5 and 7 in the surrounding region.

In an area, if you observe seismic activeness through RIAT, the presence of seismites etc., then it becomes essential to estimate the seismic hazard based on the seismic potential of identified active seismic source(s). In the present study, a displacement of the order of 25 cm (0.25 m) has been estimated along the Kelvani fault. Based on the displacement–magnitude empirical relationship, an earthquake potential of Mw 6.2 has been estimated along this fault. The PGA distribution map of the region based on a scenario earthquake of MW 6.2 along the Kevani fault at Vs of 760 m/sec^2 and surface using site amplification factor estimated through Vs have been simulated using SFFMT. A PGA value of the order of 40 cm/s^2 to 1.360 cm/s^2 has been estimated at Vs 760 m/sec with the maximum value in the western part (towards the dipping direction) of the Kelvani Fault near Silvasa (Fig. 1.3). A site amplification of the order of 0.9–2.15 has been estimated in the study area with a maximum value in the N and NW part (near Vapi) (Fig. 1.4). The higher value of site amplification is estimated in the area covered with the sediments. A surface PGA of the order of 40 cm/sec^2 to 440 cm/sec^2 has been estimated in the study area with a maximum value in the western part of the Kelvani fault (near Silvasa and Rakholi, towards the dip direction) (Fig. 1.5).

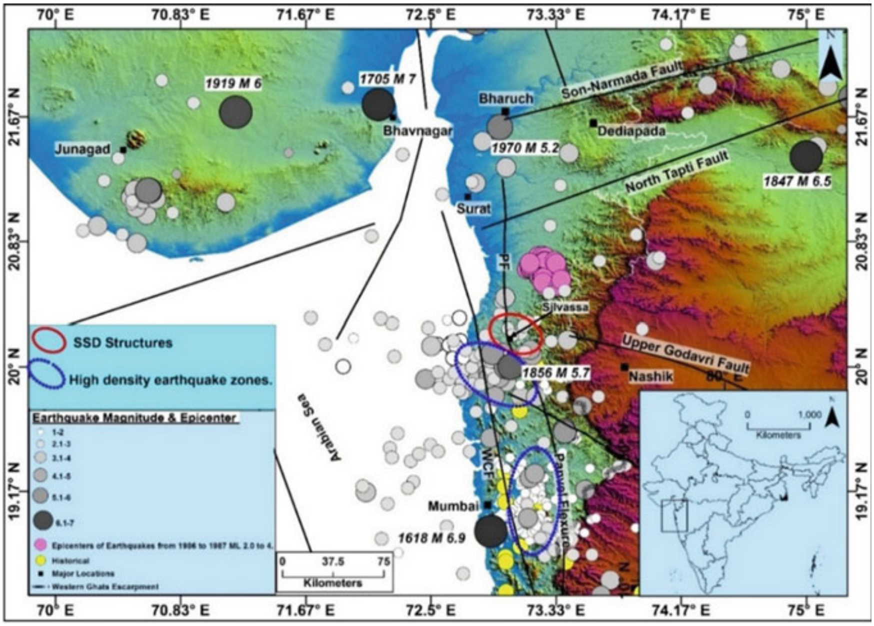

Fig. 1.10 The variation in epicentre distance of seismites (blue ellipse) with their association to 1618, 1856 earthquake (M6.9 and 5.7) affected the study area (after Kumar et al. 2020a)

1.6 Conclusion

The Dadra-Nagar Haveli and the surrounding region, in western India, have been experiencing moderate seismicity (more than 200 earthquakes ($1.0 \leq M \leq 5.7$) since 1856 including two historic events (Magnitude Ms 5 in 1935 and Magnitude Ms 5.7 in 1856). A study is conducted to map the tectonic structures in the region and their associated tectonic-geomorphic features to infer the tectonic behaviour and their impact on seismic hazard in the study area. RIAT of the watersheds of main rivers has been estimated through the geomorphic analysis SL gradient, HI, BS and VF and 03 groups ($1.3 \leq$ RIAT < 1.5 in class II with high activities, $1.5 \leq$ RIAT < 1.8 in class III—with moderate activities, and $1.8 \leq$ RIAT in class IV—with low activities, have been found in the study area indicating it a seismically active region. The study area falls within the Panvel seismic zone with the presence of faults with slickenside bearing planes, shear zones with brittle behaviour, extensional features and deformed dykes suggesting that the study area has faced neotectonic activities and is still active seismically. Through geological fieldwork, the evidence of past major seismic events (>5.5) is also found well preserved in the form of SSDS/seismites in quaternary sediments. The extent and dimension of these seismites indicate that the mechanism to trigger these and forces driven for the source of these structures were shock waves by an earthquake. The maximum moment magnitude of Mw 6.2 has been estimated based on the maximum displacement recorded along the normal active fault mapped in the study area (Kelvani Fault), which trends N170°–N350°, with a sharp dip of 72° in the SW direction. The seismic hazard assessment of the area considering scenario earthquake of Mw 6.2 along this fault located east of Silvasa city has been estimated using the Stochastic Finite Fault Modelling simulation technique. A maximum PGA of the order of 360 cm/sec^2 has been estimated at the EBR with the Vs of 760 m/sec and 440 cm/sec^2 has been estimated at the surface level with a maximum site amplification factor of 2.15 in the area.

References

Acharya HK (1979) Regional variations in the rupture-length magnitude relationships and their dynamical significance. Bull Seismol Soc Am 69(6):2063–2084

Acharya SK, Kayal JR, Roy A, Chaturvedi RK (1998) Jabalpur earthquake of May 22, 1997: constraint from aftershock study. J Geol Soc India 51(3):295–304

Albee AL, Smith JL (1966) Earthquake characteristics and fault activity in southern California. Eng Geol South Calif 1:9–34

Allen JRL (1977) The possible mechanics of convolute lamination in graded sand beds. Jour Geol Soc London 134(1):19–31

Allen JRL (1982) Sedimentary structures, their character and physical basis, vol 1. Elsevier

Allen TI, Wald DJ (2009) On the use of high-resolution topographic data as a proxy for seismic site conditions (VS 30). Bull Seismol Soc Am 99(2A):935–943

Alfaro P, Delgado J, Estévez A, Molina J, Moretti M, Soria J (2002) Liquefaction and fluidization structures in Messinian storm deposits (Bajo Segura Basin, Betic Cordillera, southern Spain). Int J Earth Sci 91(3):505–513

Alfaro P, Estevez A, Moretti M, Soria MJ (1999) Structures sédimentaires de déformation interprétées comme seismites dans le Quaternaire du bassin du Bas Segura (Cordillère bétique orientale). Comptes Rendus de l'Academie de Sciences. Serie IIa. Sciences De La Terre Et Des Planetes 328:17–22

Anderson EM (1951) The dynamics of faulting and dyke formation with applications to Britain. Hafner Pub. Co

Anderson JG, Hough SE (1984) A model for the shape of the fourier amplitude spectrum of acceleration at high frequencies. Bull Seismol Soc Am 74:1969–1993

Anketell JM, Cegła J, Dżułyński S (1970) On the deformational structures in systems with reversed density gradients. In Annales societatis geologorum poloniae, vol 40, no 1, pp 3–30

Argles TW (2010) Recording structural information. In: Coe AL (ed) Geological field techniques. Blackwell Publ, London, pp 163–191

Atkinson GM, Boore DM (1995) Ground motion relations for eastern North America. Bull Seismol Soc Am 85:17–30

Auden JB (1949) Dykes in western India-A discussion on their relationships with the Deccan Traps. Trans Nat Inst Sci India 3:123–157

Balkema AA (1997) Handbook on liquefaction remediation of reclaimed land. Port and Harbour Research Institute

Bansal BK, Gupta S (1998) A glance through the seismicity of peninsular India. J Geol Soc India 52:67–80

Bhattacharya SN, Ghose AK, Suresh G, BaidyaPR, Saxena RC (1997) Source parameters of Jabalpur earthquake of 22 May 1997. Curr Sci 855–863

Bhattacharya HN, Bandyopadhyay S (1998) Seismites in a Proterozoic tidal succession, Singhbhum, Bihar, India. Sed Geol 119:239–252

Biswas SK (1982) Rift basins in western margin of India and their hydrocarbon prospects with special reference to Kutch basin. AAPG Bull 66(10):1497–1513

Biswas SK (1987) Regional tectonic framework, structure and evolution of the western marginal basins of India. Tectonophysics 135(4):307–327

Bodin P, Malagnini L, Akinci A (2004) Ground-motion scaling in the Kachchh basin, India, deduced from aftershocks of the 2001 Mw 7.6 Bhuj earthquake. Bull Seismol Soc Am 94:1658–1669

Bonilla MG, Buchanon JM (1970) Interim report on worldwide historical surface faulting, US Geol Surv Open-file-report 70–34

Boore DM (1983) Stochastic simulation of high-frequency ground motions based on seismo537 logical models of the radiated spectra. Bull Seism Soc Am 538 73(6):1865–1894

Boore DM, Atkinson CM (1987) Stochastic prediction of ground motion and spectral response parameters at hard rock sites in eastern North America. Bull Seism Soc Am 77:440–467

Boore DM, Joyner (1997) Site amplification for generic rock sites. Bull Seism Soc Am 87(2):327–341

Brandes C, Tanner DC (2012) Three-dimensional geometry and fabric of shear deformation-bands in unconsolidated Pleistocene sediments. Tectonophysics 518:84–92

Bull WB (1977) The alluvial-fan environment. Prog Phys Geogr 1(2):222–270

Bull WB (2007) Tectonic geomorphology of mountains: a new approach to paleoseismology. John Wiley & Sons

Bull WB, McFadden LD (2020) Tectonic geomorphology north and south of the Garlock fault, California. In Geomorphology in arid regions, pp 115–138. Routledge

Calvo JP, Rodriguez Pascua M, Martin Velazquez S, Jimenez S, Vicente GD (1998) Microdeformation of lacustrine laminite sequences from Late Miocene formations of SE Spain: an interpretation of loop bedding. Sedimentology 45(2):279–292

Cancani A (1904) Sur l'emploi d'une double ´echelle sismique des intensit´es, empirique et ab571 solue. Gerlands Beitr z Geophys 2:281–283, Cited in Gutenberg and Richter 572 (1942)

Chandra U (1977) Earthquakes of peninsular India-A seismotectonic study. Bull Seismol Soc Am 67(5):1387–1413

Chinnery MA (1969) Earthquake magnitude and source parameters. Bull Seismol Soc Am 59(5):1969–1982
Chopra S, Kumar D, Rastogi BK (2010) Estimation of strong ground motions for 2001 Bhuj (M w 7.6), India earthquake. Pure Appl Geophys 167(11):1317–1330
Chopra S, Kumar D, Rastogi BK, Choudhary P, Yadav RBS (2012) Deterministic seismic scenario in Gujarat, India. Nat Haz 60:1157–2117
Chopra S, Kumar D, Rastogi BK, Choudhury P, Yadav RBS (2013) Estimation of seismic hazard in Gujarat region. India 65:1157. https://doi.org/10.1007/s11069-012-0117-5
Coppersmith KJ (1991) Seismic source characterization for engineering seismic hazard analysis: In Proceedings of 4th international conference on seismic zonation, Vol I, Earthquake engineering research institute, Oakland, California, 3–60
Courtillot V, Besse J, Vandamme D, Montigny R, Jaeger JJ, Cappetta H (1986) Deccan flood basalts at the Cretaceous/Tertiary boundary? Earth Planet Sci Lett 80(3–4):361–374
Cox KG (1988) Inaugural address In: Subbarao KV (ed) Deccan flood basalts. Geol Soc India Mem 10:15–22
Cox RT (1994) Analysis of drainage-basin symmetry as a rapid technique to identify areas of possible Quaternary tilt-block tectonics: an example from the Mississippi Embayment. Geol Soc Am Bull 106(5):571–581
Dalrymple RW (1979) Wave-induced liquefaction: a modern example from the Bay of Fundy. Sedimentology 26:835–844
Darragh RB, Bolt BA (1987) A comment on the statistical regression relation between earthquake magnitude and fault rupture length
Dikshit KR (1970) Polycyclic landscape and the surfaces of erosion in the Deccan Trap country with special reference to upland Maharashtra. Nat Geogr J India 16(3–4):236–252
Doblas M (1998) Slickenside kinematic indicators. Tectonophysics 295(1–2):187–197
Dole G, Peshwa VV, Kale VS (2000) Evidence of a Palaeoseismic event from the Deccan Plateau Uplands. J Geol Soc India 56:547–555
Dole G, Peshwa VV, Kale VS (2002) Evidences of neotectonism in quaternary sediments from Western Deccan Upland Region, Maharashtra. Memoir Geol Soc India 49:91–108
Guhman AI, Pederson DT (1992) Boiling sand springs, Dismal River, Nebraska: agents for formation of vertical cylindrical structures and geomorphic change. Geology 20:8–10
Hack JT (1973) Stream-profile analysis and stream-gradient index. J Res US Geol Surv 1(4):421–429
Hadley DM, Helmberger DV (1980) Simulation of strong ground motions. Bull Seism Soc Am 70:617–630
Hartzell SH (1978) Earthquake aftershocks as green functions. Geophys Res Lett 5:1–4
Hartzell SH (1982) Simulation of ground accelerations for May 1980 Mammoth Lakes, California earthquakes. Bull Seism Soc Am 72:2381–2387
Holzer TM, Clark MM (1993) Sand boils without earthquakes. Geology 21:873–876
Housner GW (1947) Characteristics of strong-motion earthquakes. Bull Seism Soc A 37(1):19–31
Hutchings L (1985) Modeling earthquakes with empirical green's functions (abs). Earthq Notes 56:14
Irikura K, Muramatu I (1982) Synthesis of strong ground motions from large earthquakes using observed seismograms of small events. Proceedings of the 3rd international microzonation conference, Seattle, pp 447–458
Irikura K (1983) Semi Empirical estimation of strong ground motion during large earthquakes. Bull Disaster Prev Res Inst (kyoto Univ.) 33:63–104
Irikura K (1986) Prediction of strong acceleration motion using empirical green's function. In: Proceedings of 7th Japan earthquake engineering symposium, pp 151–156
Irikura K, Miyake H (2011) Recipe for predicting strong ground motion from crustal earthquake scenarios. Pure Appl Geophys 168(1–2):85–104

Jade S, Shrungeshwara TS, Kumar K, Choudhury P, Dumka RK, Bhu H (2017) India plate angular velocity and contemporary deformation rates from continuous GPS measurements from 1996 to 2015. Sci Rep 7:11439. https://doi.org/10.1038/s41598-017-11697-w
Jones ME, Preston RMF (1987) Deformation of sediments and sedimentary rocks. Geological Society, London, Special Publications, no 29
Jones AP, Omoto K (2000) Towards establishing criteria for identifying trigger mechanisms for soft-sediment deformation: a case study of Late Pleistocene lacustrine sands and clays, Onikobe and Nakayamadaira Basins, northeastern Japan. Sedimentology 47(6):1211–1226
Joshi A, Midorikawa S (2004) A simplified method for simulation of strong ground motion using finite rupture model of the earthquake source. J Seismolog 8:467–484
Joshi A, Singh S, Kavita G (2001) The simulation of ground motions using envelope summations. Pure Appl Geophys 158:877–901
Kale VS, Rajaguru SN (1987) Late Quaternary alluvial history of the northwestern Deccan upland region. Nature 325(6105):612–614
Kale VS, Dole G, Upasani D, Pillai SP (2016) Deccan Plateau uplift: insights from parts of Western Uplands, Maharashtra, India. Geological Society, London, Special Publications 445:11–46
Kamae K, Irikura K (1998) Source model of the 1995 Hyogo-ken Nanbu earthquake and simulation of near source ground motion. Bull Seism Soc Am 88:400–412
Kanamori H, Anderson DL (1975) Theoretical basis of some empirical relations in seismology. Bull Seismol Soc Am 65(5):1073–1095
Kanamori H (1979) A semi empirical approach to prediction of long period ground motions from great earthquakes. Bull Seism Soc Am 69:1645–1670
Kaplay RD, Kumar TV, Sawant R (2013) Field evidence for deformation in Deccan Traps in microseismically active Nanded area, Maharashtra. Curr Sci 105(8)
Kaplay RD, Babar MD, Mukherjee S, Kumar TV (2016) Morphotectonic expression of geological structures in the eastern part of the South East Deccan Volcanic Province (around Nanded, Maharashtra, India). Geol Soc London 445:317–335
Keller EA (1986) Investigation of active tectonics: use of surficial earth processes. Active Tecton 1:136–147
Keller EA, Pinter N (1996) Active tectonics, vol 338. Prentice Hall, Upper Saddle River, NJ
Kranis H (2007) Neotectonic basin evolution in central-eastern mainland Greece: an overview. Bull Geol Soc Greece 40(1):360–373
Krishnan MS (1953) The structural and tectonic history of India: Geol Surv India Mem 81:137
Krishnan MS (1982) Geology of India and Burma, 6th Edition, Satish Kumar Jain for CBS Publishers and Distributors 64:536
Kumar N, Mohan K, Dumka RK, Chopra S (2020a) Soft sediment deformation structures in quaternary sediments from dadra and nagar haveli, western India. J Geol Soc India 95(5):455–464
Kumar N, Mohan K, Dumka RK, Chopra S (2020b) Evaluation of linear structures in dadra and nagar haveli, western India: implication to seismotectonics of the study area. J Ind Geophys Union 24(2):10–21
Kumar N, Dumka RK, Mohan K, Chopra S (2022) Relative active tectonics evaluation using geomorphic and drainage indices, in Dadra and Nagar Haveli, western India. Geodesy Geodyn 13(3):219–229
Kuribayashi E, Tatsuoka F (1975) Brief review of liquefaction during earthquakes in Japan. Soils Found 15(4):81–92
Lai SP (1982) Statistical characterization of strong ground motions using power spectral density function. Bull Seism Soc Am 72:259–274
Leeder MR, Alexander J (1987) The origin and tectonic significance of asymmetrical meander-belts. Sedimentology 34:217–226
Lida K (1959) Earthquake energy and earthquake fault. J Earth Sci (7):98–107. Nagoya University
Lowe DR (1975) Water escape structures in coarse-grained sediments. Sedimentology 22:157–204

Marco S, Agnon A (1995) Prehistoric earthquake deformations near Masada, Dead Sea Graben. Geology 23(8):695–698
Matsuoka M, Midorikawa S (1994) GIS-based seismic hazard mapping using the digital national land information. Proceedings of 9th Japan Earthquake
McGuire RK (2001) Deterministic vs probabilistic earthquake hazards and risks. Soil Dyn Earthq Eng 21(5):377–384
Midorikawa S (1993) Semi empirical estimation of peak ground acceleration from large earthquakes. Tectonophysics 218:287–295
Mikumo T, Irikura K, Imagawa K (1981) Near field strong motion synthesis from foreshock and aftershock records and rupture process of the main shock fault (abs.). IASPEI 21st General Assembly, London, Canada
Mills PC (1983) Genesis and diagnostic value of soft-sediment deformation structures—a review. Sed Geol 35(2):83–104
Mohan K (2014) Seismic hazard assessment in the kachchh region of Gujarat (India) through deterministic modeling using a semi-empirical approach. Seismol Res Lett 85(1):117–125
Mohan K, Dugar S, Pancholi V, Dwivedi V, Chopra S, Sairam B (2021) Micro-seismic hazard assessment of Ahmedabad city, Gujarat (Western India) through near-surface characterization/ soil modeling. Bull Earthq Eng 19:623–656. https://doi.org/10.1007/s10518-020-01020-w
Mohan K, Rastogi B, Pancholi V, Sairam B (2017) Estimation of strong motion parameters in the coastal region of Gujarat using geotechnical data. Soil Dyn Earthq Eng 92:561–572
Mohan K, Rastogi BK, Pancholi V, Gandhi D (2018) Seismic hazard assessment at micro level in Gandhinagar (the capital of Gujarat, India) considering soil effects. Soil Dyn Earthq Eng 109:354–370
Mohan G, Surve G, Tiwari P (2007) Seismic evidences of faulting beneath and Panvel flexure. Current Sci 93:991–996
Molina JM, Alfaro P, Moretti M, Soria JM (1998) Soft-sediment deformation structures induced by cyclic stress of storm waves in tempestites (Miocene, Guadalquivir Basin, Spain). Terra Nova-Oxford 10(3):145–150
Montessus de Ballore (1911) Seismic history of southern Los Andes south of parallel 16 (In Spanish), Cervantes Barcelona press, Santiago, Chile
Moretti M, Ronchi A (2011) Liquefaction features interpreted as seismites in the Pleistocene fluvio-lacustrine deposits of the Neuquén Basin (Northern Patagonia). Sed Geol 235:200–209
Moretti M, Sabato L (2007) Recognition of trigger mechanisms for soft-sediment deformation in the Pleistocene lacustrine deposits of the Sant'Arcangelo Basin (Southern Italy): seismic shock vs. overloading. Sediment Geol 196(1–4):31–45
Moretti M (2000) Soft-sediment deformation structures interpreted as seismites in middle-late Pleistocene aeolian deposits (Apulian foreland, southern Italy). Sed Geol 135(1–4):167–179
Moretti M, Soria JM, Alfaro P, Walsh N (2001) Asymmetrical soft-sediment deformation structures triggered by rapid sedimentation in turbiditic deposits (Late Miocene, Guadix Basin, Southern Spain). Facies 44(1):283–294
Motazedian D, Atkinson GM (2005) Stochastic finite-fault modeling based on dynamic corner frequency. Bull Seismol Soc Am 95:995–1010
Muguia L, Brune JM (1984) Simulations of strong ground motions for earthquakes in the Mexicali-Imperial valley. Proceedings of workshop on strong ground motion simulation and earthquake engineering applications Pub. 85–02, Earthq. Eng. Res. Inst., Los Altos, California, 21–1–21–19
Naik PK, Awasthi AK (2003) Neotectonic activities in the Koyna River basin–a synopsis. Gondwana Geological Magazine Spl. Publication, 5:157–163
Owen G (2003) Load structures: gravity-driven sediment mobilization in the shallow subsurface. Geol Soc London Spec Publ 216(1):21–34
Owen G (1996) Experimental soft-sediment deformation: structures formed by the liquefaction of unconsolidated sands and some ancient examples. Sedimentol 43:279–293
Owen G (1987) Deformation processes in unconsolidated sands. Geol Soc London Spec Public 29(1):11–24

Purcaru GEORGE, Berckhemer H (1982) Quantitative relations of seismic source parameters and a classification of earthquakes. Tectonophysics 84(1):57–128
Ramesh DS, Estabrook CH (1998) Rupture histories of two stable continental region earthquakes of India. J Earth Syst Sci 107(3):225
Renne PR, Sprain CJ, Richards MA, Self S, Vanderkluysen L, Pande K (2015) State shift in Deccan volcanism at the Cretaceous-Paleogene boundary, possibly induced by impact. Science 350(6256):76–78
Rao BR, Rao PS (1984) Historical seismicity of peninsular India. Bull Seismol Soc Am 74(6):2519–2533
Rao DT, Jambusaria BB, Srivastava S, Srivastava NP, Hamid A, Desai BN, Srivastava HN (1991) Earthquake swarm activity in south Gujarat. Mausam 42(1):89–98
Rao NP, Tsukuda T, Kosuga M, Bhatia SC, Suresh G (2002) Deep lower crustal earthquakes in central India: inferences from analysis of regional broadband data of the 1997 May 21, Jabalpur Earthquake. Geophys J Int 148(1):132–138
Raj R, Bhandari S, Maurya DM, Chamyal LS (2003) Geomorphic indicators of active tectonics in the Karjan River Basin, Lower Narmada Valley, Western India. J Geol Soc India 62:739–752
Rajendran CP (1997) Deformational features in the river bluffs at Ter, Osmanabad district, Maharashtra: evidence for an ancient earthquake. Curr Sci 72(10):750–755
Rossetti DDF (1999) Soft-sediment deformation structures in late Albian to Cenomanian deposits, São Luís Basin, northern Brazil: evidence for palaeoseismicity. Sedimentology 46(6):1065–1081
Saikia CK (1993) Ground motion studies in great Los Angles due to Mw = 7.0 earthquake on the Elysian thrust fault. Bull Seism Soc Am 83:780–810
Saikia CK, Herrmann RB (1985) Application of waveform modelling to determine focal mechanisms of four 1982 Miramichi aftershocks. Bull Seismol Soc Am 75:1021–1040
Schwartz DP, Coppersmith KJ (1986) Seismic hazards: new trends in analysis using geologic data (No. DOE/ER/12018--T10)
Schwartz DP (1988) Paleoseismicity and neotectonics of the Cordillera Blanca fault zone, northern Peruvian Andes. J Geophys Res Solid Earth 93(B5):4712–4730
Seed HB, Idriss IM (1971) Simplified procedure for evaluating soil liquefaction potential. Jour Soil Mech Found Division 97:1249–1273
Seilacher A (1984) Sedimentary structures tentatively attributed to seismic events. Mar Geol 55(1–2):1–12
Seilacher ADOLF (1969) Fault-graded beds interpreted as seismites. Sedimentology 13(1–2):155–159
Sheth HC (1998) A reappraisal of the coastal Panvel flexure, Deccan Traps, as a listric-fault controlled reverse drag structure. Tectonophysics 294:143–149
Sims JD (1973) Earthquake-induced structures in sediments of Van Norman Lake, San Fernando, California. Science 182(4108):161–163
Sims JD (1975) Determining earthquake recurrence intervals from deformational structures in young lacustrine sediments. Tectonophysics 29(1–4):141–152
Singh SK, Bazan E, Esteva L (1980) Expected earthquake magnitude from a fault. Bull Seismol Soc Am 70(3):903–914
Strahler AN (1952) Hypsometric (area-altitude) analysis of erosional topography. Geol Soc Am Bull 63(11):1117–1142
Tandon AN, Chatterjee SN (1968) Seismicity studies in India. MAUSAM, 19(3):273–280
Tocher D (1958) Earthquake energy and ground breakage. Bull Seismol Soc Am 48(2):147–153
Utsu T (1970) Aftershocks and earthquake statistics (1): Some parameters which characterize an aftershock sequence and their interrelations. J Fac Sci Univ, Hokkaido University, Series 7, Geophys 3(3):129–195
Vanneste K, Meghraoui M, Camelbeeck T (1999) Late Quaternary earthquake-related soft-sediment deformation along the Belgian portion of the feldbiss fault, Lower rhine graben system. Tectonophysics 309(1–4):57–79

Waltham AC, Fookes PG (2003) Engineering classification of karst ground conditions. Quarterly Jour Engg Geol Hydrogeol 36:101–118
Watts AB, Cox KG (1989) The Deccan Traps: an interpretation in terms of progressive lithospheric flexure in response to a migrating load. Earth Planet Sci Lett 93:85–97
Whiteside, P (1986) Discussion on 'Large-scale toppling within a sackung type deformation at Ben Attow, Scotland'by G. Holmes and JJ Jarvis. Quart J Eng Geol Hydro 19(4):439–439
Wells DL, Coppersmith KJ (1994) New empirical relationships among magnitude, rupture length, rupture width, rupture area, and surface displacement. Bull Seismol Soc Am 84:974–1002
Widdowson M, Cox KG (1996) Uplift and erosional history of the Deccan Traps, India: Evidence from laterites and drainage patterns of the Western Ghats and Konkan Coast. Earth Planet Sci Lett 137(1–4):57–69
Widdowson M (1997) Tertiary palaeosurfaces of the SW Deccan, Western India: implications for passive margin uplift. Geol Soc London Spec Publ 120(1):221–248
Wyss M (1979) Estimating maximum expectable magnitude of earthquakes from fault dimensions. Geology 7(7):336–340
Yu G (1994) Some aspects of earthquake seismology: slip portioning along major convergent plate boundaries: composite source model for estimation of strong motion and nonlinear soil response modeling. PhD thesis, University of Nevada
Yu G, Khattri KN, Anderson JG, Brune JN, Zeng Y (1995) Strong ground motion from the Uttarkashi earthquake, Himalaya, India, earthquake: comparison of observations with synthetics using the composite source model. Bull Seismol Soc Am 85:31–50
Zeng Y, Anderson JG, Su F (1994) A composite source model for computing realistic synthetic strong ground motions. Geophys Res Lett 21:725–728